Microchemical Journal 196 (2024) 109575

Contents lists available at ScienceDirect

Microchemical Journal

journal homepage: www.elsevier.com/locate/microc

A combined study of gamma spectrometry and inductively coupled plasma spectroscopy reveals persistent anthropogenic radioactive pollution on Deception Island, Antarctica

E. Abás [a], C. Marina-Montes [a], C. Pérez-Marín [b], J. Puimedón [b], J. Anzano [a,*]

[a] Laser Lab, Chemistry & Environment Group, Department of Analytical Chemistry, Faculty of Sciences, University of Zaragoza. Pedro Cerbuna 12, 50009 Zaragoza, Spain
[b] LABAC, Centro de Astropartículas y Física de Altas Energías (CAPA), Universidad de Zaragoza, Pedro Cerbuna 12, 50009 Zaragoza, Spain

ARTICLE INFO

Keywords:
Antarctic region
Environmental studies
Radionuclides
ICP-MS
Gamma spectrometry

ABSTRACT

A comprehensive measurement of the concentrations of natural and anthropogenic radionuclides in soil, water, and air was carried out during the austral summer Antarctic campaign 2018–2019 in different locations around the Spanish Research Station "Gabriel de Castilla" (Deception Island, South Shetland Islands, Antarctica). Limited information is available on radionuclide contamination in the Antarctic region. This study was conducted to evaluate Deception Island's capacity to remove and self-clean its environment. For this reason, samples from soil, water, and air were collected and analysed by gamma spectrometry, inductively coupled plasma mass spectrometry, and inductively coupled plasma optical emission spectroscopy. The obtained results revealed significant levels of ^{210}Pb and anthropogenic ^{137}Cs, in soil samples close to old human settlements and facilities. In terms of water samples, although more renovation was expected than Antarctic soil, human impact was confirmed again since significant levels of both anthropogenic radionuclides, ^{137}Cs and ^{60}Co, are still detectable in old hunting areas. Air quality studies are not totally conclusive because the obtained results are significantly higher than those previously reported, a fact that potentially points to resuspension processes.

1. Introduction

The Antarctic is one of the least polluted, cleanest, most pristine, and isolated places on Earth [22]. Harsh environmental conditions make this continent a complicated place for developing both, ecological and human activities. Therefore, Antarctic's species diversity is low, and they are mostly located on ice-free soils [41].

The Antarctic treaty [1] signed by 56 countries, establishes Antarctica as a scientific preserve and bans nuclear activity on this continent [1]. However, although the treaty and its isolation by the Southern Ocean from other regions, Antarctica, and among others, its soils are affected by remote natural and anthropogenic radioactivity. These radionuclides are transported from thousands of kilometres away to Antarctica by air masses and sea currents.

Radioactive fallout in the Antarctic region occurred mostly in the 1960s, since most the nuclear explosions occurred during that period [23]. Most atmospheric nuclear weapons have been tested in the Northern Hemisphere, while some French and British nuclear tests have occurred in the Southern Hemisphere (southern Pacific, Australia and Indian Ocean). In addition, radionuclide aerosols were released in 1986 and 2011, in the Chernobyl and Fukushima accidents, respectively [2,40]. It is remarkable that the behaviour of fission products depends on the latitude, altitude, and season when they are released [34]. For example, only those radionuclides present in the stratosphere, can reach the Southern Hemisphere from tests in the Northern Hemisphere, owing to the higher altitudes and to the more powerful detonations. In these terms, it can be inferred that the concentrations of anthropogenic radionuclides in Antarctica are dependent on the conditions of the operating long-range transport process. Once the radionuclides reach Antarctica, their deposition processes are also controlled by meteorological conditions such as wind current, rain, and so on, but they are not completely understood yet [12].

Since the period when the radionuclides arrived in Antarctica is well-defined, these values have been used as reference levels in snow samples and, are currently used in glaciological studies. Snow samples are commonly used for such studies [3,32,48], but in this investigation, we

* Corresponding author.
E-mail address: janzano@unizar.es (J. Anzano).

https://doi.org/10.1016/j.microc.2023.109575
Received 10 July 2023; Received in revised form 4 October 2023; Accepted 12 October 2023
Available online 2 November 2023

have analysed samples of different nature to combine different pieces of information on the radionuclides in Antarctica. Thus, several air, water, and soil samples were collected and analysed by gamma spectrometry.

Different techniques can be used for radioactivity measurement, but gamma spectrometry is increasingly important in environmental radionuclide dispersion studies. The most important sources of natural radioactivity are ^{40}K and the natural series heading of ^{232}Th, ^{238}U and ^{235}U, and their descendants. These natural radionuclides like ^{232}Th have been studied mostly in the last years, in different Antarctic regions, and a huge difference was observed. In the beginning, Tubertini et al. published low values of ^{232}Th (12–81 Bq/kg) in 1995; however, an increasing tendency has been observed since Bakshi *et al.* in 2017 found 228–216 Bq/kg in the Grovnes region [4]. A recent study conducted in the Larsemann Hills region showed a ^{232}Th activity of 199 Bq/kg [30].

Additionally, because of the nuclear tests performed in this area and, some others, artificial radionuclides can be potentially found. In this aspect, some traces of ^{137}Cs and ^{60}Co can be detected because of their long half-lives and their common use in medical and industrial activities. The activity of these artificial radionuclides is expected to decrease; however, a great dependence on the region is observed. In Byers Peninsula, ^{137}Cs activities of 1.2 ± 1.1 Bq/kg in 2005 were found [27], whereas values of 6.2 ± 1.2 Bq/kg were recorded in King George station or 3.16 ± 0.34 Bq/kg in Elephant Island in 1992 [15].

Measurement of artificial and natural radionuclides in samples from the continental and marine environments of Antarctica is needed and important to evaluate the impact of human activities in this considered free-pollution location. A complete study of the possible radionuclide pollution in Antarctica is needed because soil, water, and air are highly linked.

The soil environment plays a critical ecological role in flora and fauna, and in the disintegration of radionuclides that occur in it. These radioactive concentrations can be transferred to Antarctic ecosystems, negatively affecting them. Thus, the investigation of isotopic elements in soils plays an important role in understanding the radioactivity impacts on Antarctic ecosystems. Besides, since the primordial radionuclides, such as ^{40}K, ^{238}U, and ^{232}Th, are found in most types of soils, they can be easily resuspended into the lower troposphere, and consequently detected in air filters. The same mechanism can be followed by other anthropogenic radionuclides, such as ^{137}Cs. To continue the whole cycle, using deposition processes among others, airborne radionuclides return to the soil or to the water ecosystem.

This study aims to provide further information on the concentration distribution, and association of long-lived artificial radionuclides in the Antarctic environment, particularly on Deception Island. Nowadays, there is almost no existing information on these topics and more precisely on Deception Island, something that could be related to the lack of ice and snow-free areas (less than 1 % of the total surface), in Antarctica.

The establishment of the concentration of artificial and natural radionuclides, can help us to understand the arrival and deposition processes of other artificial or natural radionuclides, and consequently, to elucidate the effectiveness and capacity of the removal of Antarctica.

2. Materials and methods

2.1. Site description

Soil and water samples were collected during the 2018–2019 campaign and, air samples during the 2019–2020 campaign. The scientists were based at the Spanish Antarctic Research station "Gabriel de Castilla". Volcanic Deception Island is located 120 km north of the Antarctic Peninsula and is part of the South Shetland Islands archipelago (Fig. 1). In the early 20th century, Deception Island was known for 30 years for its whaling industry located in Whalers Bay. Nowadays, the island is used for scientific purposes with a Spanish (Gabriel de Castilla) and an Argentinian (Decepción) research bases; and as a tourist destination, with Whalers Bay being the second most visited place in Antarctica in the summer 2016–2017 [20].

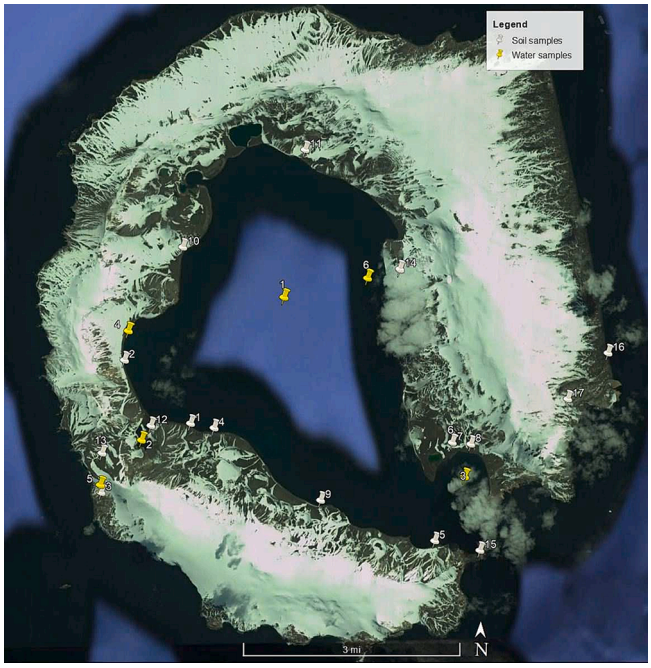

Fig. 1. Water and soil sample locations on Deception Island. *The low-volume sampler for air samples is located at the same coordinates as point 4 for water samples*.

2.2. Sampling technique, gamma spectrometry, and data analysis

A total of 17 soil samples were collected from the island at different locations (from Dec. 2018 to Feb. 2019). Each sample was collected over the area of interest in high-density polyethylene pots using sterile shovel and nitrile gloves. At each sampling point, 200 g of soil was taken from the 0–5 cm layer in an area of 1 m^2.

In the same Spanish Antarctic campaign, 6 water samples were collected over different water masses of the island (lakes and sea). At each sampling point, 0.5 L of water was taken from the 30 cm water surface in high density polyethylene pots using two pairs of nitrile gloves. Prior to the final sampling, water was discarded three times. In both soil and water sampling, GPS coordinates of the exact sample location were recorded in the field and used to develop the map shown in Fig. 1.

Atmospheric aerosol particles were collected during the austral summer (from December 2020 to February 2021) at Deception Island, at the Spanish Antarctic Research base "Gabriel de Castilla" (62°58′45.9″ S, 60°39′41.5″ W). A total of 6 samples were collected using circular quartz filter paper of 47 mm diameter (Munktell) by a Derenda LVS 3.1 low volume sampler (2.3 m^3/h), during 24 h. After that, all filters were then placed by hand in sterile Petri dishes using sterile tweezers and nitrile gloves. Mass concentration was obtained from gravimetry, following the European standard [39].

To identify the radionuclides in the samples, gamma spectrometry measured gamma radiation energies with a resolution of the order of 0.1 %. This technique is widely used for the quantitative analysis of the concentration of radioactive isotopes in samples because, most of them emit gamma radiation. Gamma spectrometry was performed at the Laboratorio de Bajas Actividades (LABAC) of the University of Zaragoza (Spain). Each sample was weighed, and the soil or water was placed in cylindrical plastic containers of 120 mL (soil) and 130 mL (water) for the analysis; the air filters were measured in their Petri dishes. Two low background Canberra High Purity Germanium (HPGe) detectors were used. The first one was a coaxial-extended range GX4018, 43.7 %

relative efficiency for 1.33 MeV and the second one was a coaxial reverse-electrode GR3520, 31.7 % relative efficiency for 1.33 MeV.

Samples were measured for 60 h. The detector efficiencies were determined in 2-h time measurements. Two 120 mL and 130 mL containers filled with soil and deionized water, respectively, were spiked with small activities of certified gamma emitters: ^{210}Pb, ^{241}Am, ^{137}Cs and ^{60}Co for soil and ^{241}Am, ^{137}Cs, ^{60}Co for water. We also used the latter three radionuclides to spike a 4-mm filter to measure the efficiency of the collected aerosols. We estimated three blanks, one per sample type, by measuring for 60 h empty containers and filters of the same geometry and material as that used to house the soil, water, and aerosols.

The energies and counting rate of the different gamma rays observed in the spectrum were analysed with software developed by the research laboratory itself. As a result, the radioisotopes contained in the sample were identified and their specific activity (Bq/kg or Bq/L) in Becquerel per unit of sample mass analysed. All measurement uncertainties are at 68 % confidence level.

The following natural and artificial radionuclides were analysed in Antarctic samples:

- Natural isotopes: ^{40}K, ^{208}Tl, ^{212}Pb, ^{212}Bi, ^{228}Ac, ^{210}Pb, ^{214}Bi, ^{214}Pb, ^{226}Ra, ^{234}Th.
- Artificial isotopes: ^{60}Co and ^{137}Cs.

Additionally, ICP-MS and ICP-OES analyses were conducted as a reference technique for the different elements detected by gamma spectrometry. The chemical characterization of the samples was perfomed following the analytical procedure published by Querol and coworkers [37]. A small 3/16 section (~33.12 cm^2) of each filter was cut and digested with 2.5 mL of HNO_3 at 65 % and, 5 mL of HF at 40 % to dissolve the potentially abundant species in soil samples such as aluminosilicates, carbonates, sulphur, etc. Then, 2.5 mL of 60 % $HClO_4$ was added to dissolve the organic matter. For quality assurance and control, blank filter analyses and NIST-1663b (fly ash, Standard Reference Material) were performed as a reference. External calibration was performed in ICP-MS using different concentrated solutions (0.25, 0.5, 1, 2, 5 and 10 ppb as well as a HNO_3 5 % blank), and ^{103}Rh was used as an internal standard to minimize the possible fluctuations of the plasma. External calibration was performed in ICP-OES using elemental standards solutions (0.05, 0.5, 1, 2, 5, 10, and 25 ppm and a HNO_3 5 % blank). The minimum detectable concentration (MDC) obtained for most of the elements ranged from 0.01 to 8.5 μg/g for ICP-MS.

In order to discern potential origins, both natural and human-induced, at the sampling site, a ten-day analysis of air-mass backward trajectories was conducted, terminating at a height of 600 m above ground level (AGL). This altitude was selected due to the island's distinctive circular topography, with its highest peak, Mount Pond, reaching an elevation of 542 m. Multiple trajectory models were employed in this investigation. For this particular study, the trajectories were computed using the NOAA HYSPLIT4 (Hybrid Single Particle Lagrangian Integrated Trajectory) model. This choice was made after a careful evaluation of available options, with preference given to GDAS 1 degree (Global Data Assimilation System) meteorological data sourced from the National Weather Service's National Centre for Environmental Prediction (NCEP). This model was deemed the most suitable due to its coverage of the study area and higher resolution compared to other models that did not encompass the specific region under investigation.

3. Results and discussion

3.1. Radionuclide activity studies in soil samples

Natural radionuclides are expected to be found in our samples (^{40}K and the radioactive series of ^{238}U, ^{232}Th and a minor amount of ^{235}U). Additionally, not only the main element of the different branches of the radioactive chain, such as ^{238}U or ^{226}Ra, but also the following elements from its radiological series.

The secular equilibrium between radionuclides of the natural decay series can be broken due to geochemical processes that move the different atoms from their production area to other far areas. The high mobility of uranium with respect to radium gives activity ratios $^{226}Ra/^{238}U \neq 1$ [9], and under typical environmental conditions, the order of mobility is U > Ra > Th [5] and references therein. The mobilization and fractionation can be produced in the near-surface environment by the different chemical characteristics of the Th and U compounds, although the disequilibrium has also been observed in igneous rocks unaffected by erosion or sedimentation. This natural imbalance is very useful for studying terrestrial and marine environments [21,28]. The disequilibrium of ^{210}Pb in soils can be produced by the escape of ^{222}Rn (daughter of ^{226}Ra) to the atmosphere [11,18,29]. Thenceforth, the activity of ^{210}Pb (descendant of ^{222}Rn) decreases in the emanation zone, but it increases in the soil surface of other zones where airborne ^{210}Pb is deposited [25]. The level of ^{210}Pb derived from the decay of ^{226}Ra is called *supported* ^{210}Pb, whereas the additional activity is called *unsupported* ^{210}Pb.

In addition to natural processes, human activities, mainly the metallurgical industry, can produce disequilibrium in the radioactive series in the ores. The extraction of the desired metals requires physical and chemical procedures that remove radionuclides with different efficiencies according to the properties of the corresponding elements, breaking down the chain equilibrium [36].

The measurement of the gamma-emitting nuclei from each radiological series provides a general and useful view of the series equilibrium. The disequilibrium can be observed by gamma spectrometry in the ^{238}U series (Fig. 2) if the breakdown affects long-lived radionuclides such as ^{226}Ra ($T_{1/2}$ = 1600 y) or ^{210}Pb ($T_{1/2}$ = 22.2 y). For this reason, ^{210}Pb, ^{214}Bi, ^{214}Pb and ^{234}Th have been measured by gamma spectrometry to evaluate the equilibrium of the ^{238}U radioactive series; the obtained results are collected and expressed as mean ± SEM in Table 1.

The activity of the parent nucleus, ^{238}U, was evaluated through the two unresolved gamma lines at 92.4 and 92.8 keV emitted after the ^{234}Th decay; the intensity used for the sum peak was 4.77 % [14]. The immobility of thorium in the soil surface [9,10], and the short half-life of ^{234}Th, 24 days [7], guarantee that ^{234}Th activity is a good estimate of ^{238}U activity, even in the case of an *in situ* measurement [25]. In this study, the ten months elapsed between sampling and measurement assure the ^{234}Th equilibrium. The ^{226}Ra activity can be estimated from the weighted mean of the activities of the short-lived descendants, ^{214}Pb and ^{214}Bi, because their equilibrium with ^{226}Ra was maintained in the airtight container of the samples to prevent the outgassing of ^{222}Rn. The specific activities of ^{234}Th, ^{214}Pb, and ^{214}Bi (Table 1) are equal within uncertainties at 3σ level[1] for the 17 samples, showing that ^{238}U and ^{226}Ra are in equilibrium within our precision.

On the other hand, we used the 186-keV peak, the addition of 185.7 keV from ^{235}U, and 186.2 keV from ^{226}Ra, as cross-checking of ^{238}U−^{226}Ra equilibrium. Assuming that the isotopic abundances of ^{235}U and ^{238}U are natural, 0.72 % and 99.28 %, respectively [7], and that ^{238}U and ^{226}Ra are in equilibrium, 57.5 % of the area of the observed 186 keV peak comes from ^{226}Ra. Therefore, the ^{226}Ra activity calculated from this fraction (Table 1, last column) should be equal to the activities of ^{234}Th, ^{214}Pb and ^{214}Bi of Table 1 because it is very unlikely that the Antarctic soil contains enriched or depleted uranium. As shown in Table 1, the calculated activity of ^{226}Ra is consistent with the measured ^{234}Th, ^{214}Bi, and ^{214}Pb activities, and therefore the ^{238}U−^{226}Ra equilibrium and the natural uranium abundances are confirmed, within uncertainties, in every soil sample. Note that if ^{234}Th, ^{214}Pb and ^{214}Bi

[1] We assume that two measures $(a \pm \sigma_a)$ and $(b \pm \sigma_b)$ are different if $|\Delta| > 3\sigma_\Delta$, where $\Delta = a - b$ and.$\sigma_\Delta = \sqrt{\sigma_a^2 + \sigma_b^2}$

$$^{238}U \xrightarrow[\alpha]{4.5\times10^{9}\ y} {}^{234}Th \xrightarrow[\beta]{27\ d} \ldots\ldots\ldots {}^{226}Ra \xrightarrow[\alpha]{1600\ y} \ldots\ldots\ldots {}^{210}Pb \xrightarrow[\beta]{22\ y} \ldots\ldots\ldots$$

Fig. 2. Beginning of the ^{238}U decay series and intermediate long-lived radionuclides ^{226}Ra and ^{210}Pb, where disequilibrium can be observed.

Table 1
Specific activities of the gamma emitters of ^{238}U decay series in soil samples. The ^{226}Ra values were calculated assuming radioactive equilibrium and natural uranium (see text).

Sample Locations	^{234}Th (Bq/kg)	^{214}Bi (Bq/kg)	^{214}Pb (Bq/kg)	^{210}Pb (Bq/kg)	Calculated ^{226}Ra (Bq/kg)
1. Area between the Argentinian and Spanish Research Bases	4.1 ± 1.2	5.8 ± 0.4	5.2 ± 0.2	4.4 ± 0.9	3.7 ± 0.7
2. Fumarole Beach	8.6 ± 2.0	5.5 ± 0.3	5.8 ± 0.3	5.6 ± 1.2	6.2 ± 1.0
3. Punta Descubierta Penguin Colony	6.2 ± 1.7	4.8 ± 0.3	5.2 ± 0.3	2.7 ± 1.0	5.7 ± 1.0
4. Surroundings of the Spanish research station "Gabriel de Castilla"	5.1 ± 0.9	6.2 ± 0.3	5.6 ± 0.2	7.9 ± 1.1	6.9 ± 1.2
5. Lobera beach	8.1 ± 2.3	6.3 ± 0.4	6.6 ± 0.3	5.2 ± 1.2	7.9 ± 1.3
6. Norwegian Aktieselskabet Hektor whaling station	4.7 ± 0.8	7.0 ± 0.3	7.2 ± 0.3	10.6 ± 1.2	6.1 ± 0.9
7. Surroundings British research station "Base B".	6.5 ± 1.4	5.3 ± 0.3	5.7 ± 0.3	11.4 ± 1.3	5.8 ± 1.0
8. Whalers Bay	5.0 ± 0.8	5.6 ± 0.3	5.2 ± 0.2	5.0 ± 1.0	4.9 ± 0.8
9. Colatinas Beach	9.4 ± 1.1	6.4 ± 0.3	6.2 ± 0.3	7.1 ± 1.0	5.7 ± 0.8
10. Obsidiana Beach	9.3 ± 1.8	8.5 ± 0.4	8.5 ± 0.4	12.8 ± 2.4	12.0 ± 2.5
11. Eruption Crater 1970	4.7 ± 0.9	7.2 ± 0.3	7.1 ± 0.3	8.1 ± 1.1	7.5 ± 0.9
12. Surroundings of the Argentinian research base	4.7 ± 1.3	5.4 ± 0.3	5.4 ± 0.3	8.1 ± 1.7	5.5 ± 1.1
13. Vapour Col	3.0 ± 0.7	4.8 ± 0.3	4.7 ± 0.2	6.1 ± 1.0	4.1 ± 0.7
14. Chilean Shelter	9.5 ± 3.1	6.4 ± 0.4	6.9 ± 0.3	7.0 ± 1.6	7.2 ± 1.5
15. Punta Entrada Penguin Colony	5.0 ± 0.9	4.4 ± 0.3	4.4 ± 0.3	5.0 ± 1.2	3.7 ± 1.0
16. Baily Head Beach	8.5 ± 1.7	7.5 ± 0.4	7.7 ± 0.3	6.5 ± 1.8	7.8 ± 1.3
17. Baily Head Col	7.8 ± 2.3	4.6 ± 0.4	5.3 ± 0.3	3.0 ± 1.1	4.9 ± 1.1

had the same activity, but the 186 keV peak cross-check failed, it would indicate an abnormal uranium isotopic content that merits further research.

The activity of ^{210}Pb, which is directly estimated from the 46.5 keV gamma ray emitted after its decay to ^{210}Bi, is equal to the activities of ^{214}Pb and ^{214}Bi, except for soil sample **7**. In this case, there is a significant (greater than 3σ) unsupported ^{210}Pb. This supplementary level of ^{210}Pb, which is usually related to the ^{210}Pb fallout accumulating in soils and sediments, is determined by subtracting the ^{226}Ra activity from the measured total ^{210}Pb activity [46]. Fig. 3 (left) plots the results of this subtraction for the 17 soil samples, showing the excess of sample **7**.

The possible disequilibrium between ^{210}Pb and ^{238}U can be checked by, comparing the activities of ^{210}Pb and ^{234}Th in Table 1. In this case, both activities are equal within uncertainties, except for soil sample **6** (Fig. 3, right). Therefore, in sample **6** there exists disequilibrium ^{238}U–^{210}Pb; although the intermediate imbalance ^{238}U–^{226}Ra and ^{226}Ra–^{210}Pb are not so clear because both are just at or below the 3σ level (Table 2). We conclude that the radioactive equilibrium of the ^{238}U series is broken in samples **6** and **7**, indicating an unsupported activity of ^{210}Pb (Table 2).

Similar studies were conducted to determine the activity of the products of ^{232}Th decay chain. There are only two long-lived radionuclides, ^{228}Ra and ^{228}Th (Fig. 4), to check the radioactive equilibrium.

The ^{228}Ra activity was estimated by gamma spectrometry of her daughter ^{228}Ac (Fig. 4) and the ^{228}Th activity with ^{212}Pb, ^{212}Bi, and ^{208}Tl at the end of the chain (Fig. 5). If the ^{232}Th chain is in secular equilibrium, the activities of ^{228}Ac, ^{212}Pb, and ^{212}Bi should be compatible with each other and that of ^{208}Tl should be 36 % of that obtained for ^{212}Pb, due to the branching ratio from ^{212}Bi to ^{208}Tl (Fig. 5).

We have not found breakage (at 3σ level) of the secular equilibrium

Table 2
Summary of disequilibria found by gamma spectrometry in samples **6** and **7** for the ^{238}U series. The nuclei used to estimate the activities of ^{238}U and ^{226}Ra are listed in parentheses.

Sample Locations	^{238}U (^{234}Th) Bq/kg	^{226}Ra (^{214}Pb & ^{214}Bi) Bq/kg	^{210}Pb Bq/kg	Unsupported ^{210}Pb Bq/kg
6. Norwegian Aktieselskabet Hektor whaling station	4.7 ± 0.8	7.1 ± 0.2	10.6 ± 1.2	3.5 ± 1.2
7. Surroundings British research station "Base B".	6.5 ± 1.4	5.5 ± 0.2	11.4 ± 1.3	5.9 ± 1.3

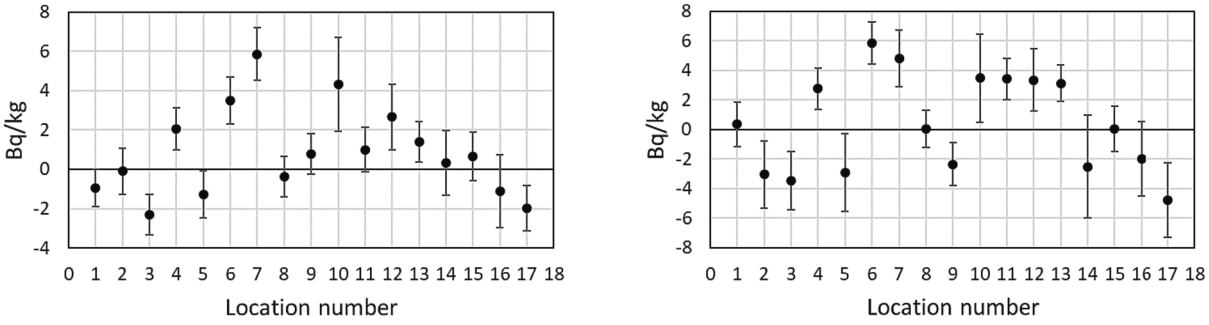

Fig. 3. Unsupported specific activity of ^{210}Pb (left) and difference between the specific activities of ^{210}Pb and ^{234}Th (right) for all soil samples.

$$^{232}Th \xrightarrow[\alpha]{1.4\times10^{10}\ y} {}^{228}Ra \xrightarrow[\beta]{5.7\ y} {}^{228}Ac \xrightarrow[\beta]{6.1\ h} {}^{228}Th \xrightarrow[\beta]{1.9\ y} \ldots\ldots\ldots \longrightarrow {}^{208}Pb$$

Fig. 4. Beginning of the ^{232}Th decay series, showing the long-lived radionuclides ^{228}Ra and ^{228}Th, where disequilibrium can be observed.

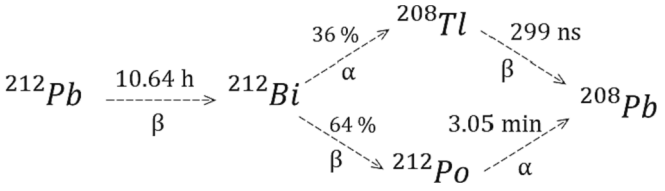

Fig. 5. Decay scheme for ^{212}Pb.

in the ^{232}Th chain in any soil sample, not even in samples **6** and **7**, where we observed disequilibrium in the ^{238}U chain. We have summarized our results in Fig. 6, plotting the activities of ^{228}Ra (^{228}Ac) and ^{228}Th (weighted mean of ^{212}Pb, ^{212}Bi and ^{208}Tl corrected by her branching ratio).

Additional studies have been conducted for the natural isotope ^{40}K (Table 3). All results are lower than the average concentration of the upper continental crust, 850 Bq/kg [19], which corresponds to the average abundance of K in the upper continental crust, 2.7 % [43]. The K content of the dominant rock at the sampling area is approximately 0.5 %, fitting well within the range of K abundance in Earth rocks, from 0.001 % for dunite or peridotite to 4.5 % for granodiorite [43].

The measurements of ^{137}Cs for all samples highlighted the impact of humans on the Antarctic region. Only in specific areas and surroundings where human settlements are or have been placed, ^{137}Cs was detected (Table 3). We have not found the other anthropogenic radionuclide searched for, ^{60}Co; its specific activity is less than 0.22 Bq/kg (95 % C.L.) for all soil samples.

As mentioned, ^{137}Cs is an artificial radionuclide, and due to its half-life of 30.1 years, it is particularly concerning [44]. In fact, it is considered an important indicator of radioactive pollution. In these terms, ^{137}Cs can persist for a long time in soils and deeply affects the human population and their food chain. ^{137}Cs can travel and be finally carried to the surface of soils by several mechanisms such as direct deposition (wet and dry) from the atmosphere, wash-off from

Table 3
Specific activities of ^{40}K and ^{137}Cs in soil samples.

Sample Locations	^{40}K (Bq/kg)	^{137}Cs (Bq/kg)
1. Area between the Argentinian and Spanish Research Bases	69.7 ± 2.6	<0.26
2. Fumarole Beach	145.3 ± 3.6	<0.22
3. Punta Descubierta Penguin Colony	129.7 ± 3.5	<0.20
4. Surroundings of the Spanish research station "Gabriel de Castilla"	153.1 ± 3.6	0.50 ± 0.05
5. Lobera beach	160.8 ± 4.1	<0.25
6. Norwegian Aktieselskabet Hektor whaling station	181.0 ± 4.3	0.40 ± 0.05
7. Surroundings British research station "Base B".	122.5 ± 3.5	0.50 ± 0.11
8. Whalers Bay	148.4 ± 3.7	<0.25
9. Colatinas Beach	175.1 ± 4.1	<0.27
10. Obsidiana Beach	210.9 ± 4.8	<0.26
11. Eruption Crater 1970	184.5 ± 4.3	<0.26
12. Surroundings Argentinian research base "Decepción"	125.7 ± 3.6	0.88 ± 0.13
13. Vapour Col	127.3 ± 3.3	<0.26
14. Chilean Shelter	153.5 ± 4.1	<0.26
15. Punta Entrada Penguin Colony	118.8 ± 3.6	<0.26
16. Baily Head Beach	185.8 ± 4.2	<0.26
17. Baily Head Col	142.9 ± 4.3	<0.26

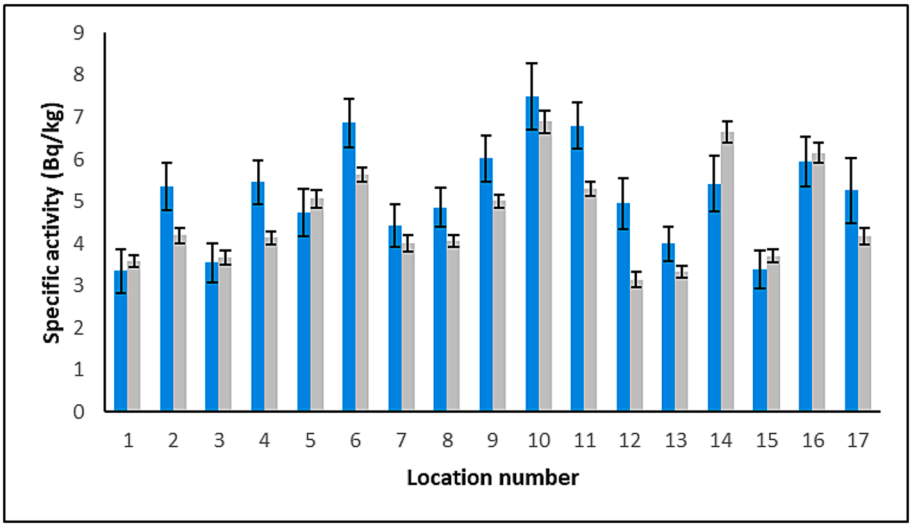

Fig. 6. Specific activities of ^{228}Ra (blue) and ^{228}Th (grey) in the soil samples. (For interpretation of the references to colour in this figure legend, the reader is referred to the web version of this article.)

vegetation, and deposition from water on floodplains and regions along the coast. Based on the sample locations, ^{137}Cs can even come from the materials used in the infrastructures themselves [49]. In addition, the adsorption of contaminated particles by organic matter, which is less mobile than inorganic matter, reduces the loss of ^{137}Cs due to erosion and can partially explain the ^{137}Cs contamination of human settlements.

Our results suggest that the ^{137}Cs fallout from the second half of the twentieth century nuclear weapon tests was low in the analysed area. They agree with previous studies estimating that the deposition of ^{137}Cs in the Antarctic was a small fraction, 0.09 % [34] or 0.08 % [35] of its total deposition in the world.

3.2. ICP-MS of soils samples

Deeper studies based on ICP-MS were performed in the samples where anthropogenic ^{137}Cs was detected (samples **4**, **6**, **7** and **12**). In samples **6** and **7**, we observed the ^{238}U chain disequilibrium. The ICP-MS (Table 4) studies were also focused on elements having natural radioactive isotopes (U, Th, K), Cs, and Pb because we detected ^{137}Cs and unsupported ^{210}Pb and, finally, Sn in sample **7** because it has the greatest concentration of ^{210}Pb, a usual contamination of tin [16]. The observed ^{137}Cs activity (Table 3) was not correlated with the caesium concentration in soils (Table 4), as expected, because ^{137}Cs is a widespread fission product.

The concentrations of U, Th, and K in soils have been converted to their corresponding specific activities (last three rows of Table 4) to deepen the study of the equilibrium of ^{238}U and ^{232}Th series (Fig. 7), because mass spectrometry provides precise measurements of the activity of both parents, with uncertainties ranging from 1 % to 3 %. Furthermore, the K concentration provides a cross-checking of gamma spectrometry because of the constant isotopic abundance of ^{40}K, (1.1668 ± 0.0008) × 10^{-4} [26]. The ^{40}K data of Table 4 and Table 3 are compatible except for sample **6**, showing a significant difference > 3σ, that can indicate some inhomogeneity in that sample because we took 200 g of soil in every location, but less than 1 g was used in ICP − MS. A small coefficient of variation of 3 % in the potassium concentration would solve the disagreement between the ^{40}K activity and the potassium concentration in sample **6.** Note that gamma spectrometry is less affected by inhomogeneity because we used approximately 150 g of sample mass in every measurement.

Table 4
ICP-MS results (μg/g) of soil samples from locations **4**, **6**, **7** and **12**. The last three rows list the specific activities (Bq/kg) of ^{40}K, ^{238}U and ^{232}Th deduced from the ICP-MS results for K, U, Th and Sn* respectively.

Element	4. Surroundings of the Spanish research station "Gabriel de Castilla"	6. Norwegian Aktieselskabet Hektor whaling station	7. Surroundings British research station "Base B"	12. Surroundings Argentinian research base "Decepción"
K (μg/g)	4798 ± 27	5274 ± 82	4318 ± 50	4282 ± 39
Cs (μg/g)	0.223 ± 0.004	0.276 ± 0.004	0.334 ± 0.007	0.224 ± 0.001
Pb (μg/g)	3.75 ± 0.15	21.73 ± 0.28	252.90 ± 0.15	15.9 ± 2.2
U (μg/g)	0.508 ± 0.007	0.529 ± 0.005	0.539 ± 0.006	0.498 ± 0.010
Th (μg/g)	1.354 ± 0.045	1.219 ± 0.013	1.85 ± 0.18	1.505 ± 0.040
Sn (μg/g)			18.8 ± 3.1	
^{40}K (Bq/kg)	148.54 ± 0.84	163.3 ± 2.5	133.7 ± 1.5	132.6 ± 1.2
^{238}U (Bq/kg)	6.272 ± 0.086	6.531 ± 0.062	6.654 ± 0.074	6.15 ± 0.12
^{232}Th (Bq/kg)	5.50 ± 0.18	4.955 ± 0.053	7.52 ± 0.36	6.12 ± 0.16

* The concentration of Sn was measured only for sample **7** (see text).

The ICP-MS values confirm the equilibrium ^{238}U−^{226}Ra (Fig. 7) in the four samples within the uncertainty (~7%) of the ^{226}Ra activity, estimated with the weighted mean of ^{214}Pb and ^{214}Bi activities. It also confirms that the unsupported activity of ^{210}Pb in samples **6** and **7** comes from the increase of ^{210}Pb, but not from a decrease in of ^{226}Ra with respect to the equilibrium value of the parent, ^{238}U. Indications of unsupported ^{210}Pb appear in samples **4** and **12**, although they are not statistically significant.

According to Equation (1)

$$\frac{^{210}Pb\ specific\ activity\ (Bq\ kg^{-1}\ of\ soil)}{Pb\ concentration\ \ (g\ kg^{-1}\ of\ soil)} = \frac{Bq\ (^{210}Pb)}{g\ (Pb)} \quad (1)$$

The unsupported activities of ^{210}Pb found in soil samples **6** and **7** (Table 2) are 161 ± 55 Bq/g (Pb) and 23 ± 5 Bq/g (Pb), respectively. The value of sample **7** is not an uncommon ^{210}Pb contamination in fresh lead [19], in solder alloys containing lead [8], or even in lead-free solders [16]. Considering that it has the highest lead mass fraction (Table 4), the result indicates that fresh lead is the main material containing ^{210}Pb. Tin is not the main element with ^{210}Pb because the mass fraction of tin in soil **7** (Table 4) would give a rather high contamination of ^{210}Pb in tin. On the other hand, in location **6**, the deposition of airborne ^{210}Pb [25] should be the main cause of the unsupported ^{210}Pb because 161 ± 55 Bq/g (Pb) would be too large if only the lead had ^{210}Pb.

The ICP-MS results for Th (Table 4) indicate that ^{232}Th activities are not compatible (Fig. 7, right) with those of their daughters ^{228}Ra (samples **6** and **7**) and ^{228}Th (all four samples). Note the gamma spectroscopy was unable to detect the disequilibrium ^{228}Ra−^{228}Th at 3σ level (Fig. 6), mainly because of the low precision of ^{228}Ra activity (~10 %). One possible explanation for samples **4**, **7**, and **12** is the loss of a large fraction of radium several years ago, but this is not possible because there is no evidence of any disruption of the ^{238}U−^{226}Ra equilibrium (Fig. 7, left). Sample **6** could be explained if a different process had produced the deficit of a large fraction of thorium; as this thorium loss does not affect the current equilibrium ^{238}U−^{226}Ra because of the ^{226}Ra long half-life (1600 y), we can understand only one of the four broken equilibria. However, all the disequilibria could be explained by inhomogeneities of 10 % (samples **4** and **6**) and 20 % (samples **7** and **12**). We performed an exploratory analysis measuring the thorium in four aliquots of sample **7,** finding a coefficient of variation of 10 % (Table 5).

The true distribution of thorium in sample **7** is unknown. If we assume it is normal, we use Eq. (2) connecting the variance,σ^2 the χ^2 distribution and the sample variance s^2 of a sample of size n, to estimate the coefficient of variation for the sample **7** within the interval [6 %, 28 %] at 90 % C.L. Probably, the thorium inhomogeneity of 20 % in sample **7** is also possible for another plausible distribution.

$$(n-1)\frac{s^2}{\sigma^2} \approx \chi^2_{n-1} \quad (2)$$

3.3. Radionuclide activity studies in water samples

The same methodology and radionuclides were measured in six water samples (Fig. 1). The results were quite different because, in water samples, we did not register any gamma emitter from the ^{238}U decay series; the minimum detectable activities (95 % C.L.) for ^{214}Bi and ^{214}Pb ranged from 0.40 to 0.71 Bq/L. The ^{232}Th daughters were only found in the snow sample, probably contaminated by soil or dust. As shown Table 6, ^{40}K was detected in the four salty water samples, whereas in the two fresh water samples (**2** and **5**), their activity values were less than the minimum detectable activity.

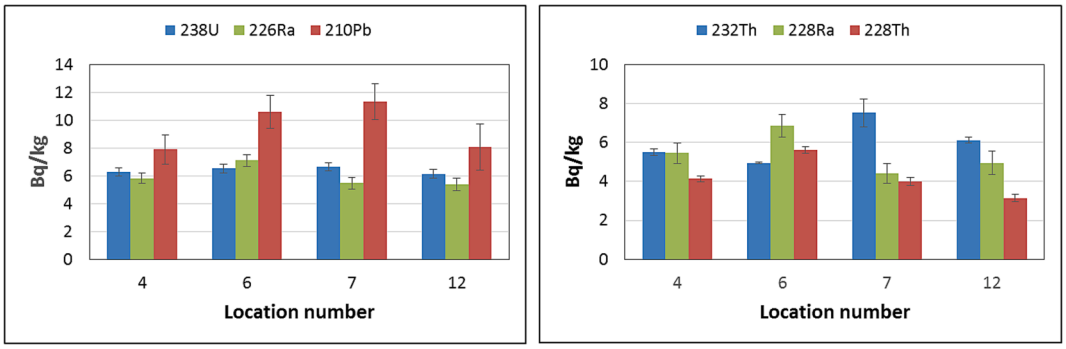

Fig. 7. Specific activities of ^{238}U and its descendants ^{234}Th, ^{226}Ra and ^{210}Pb (left) and ^{232}Th and its descendants ^{228}Ra and ^{228}Th (right). The activities of ^{238}U and ^{232}Th are deduced from ICP-MS; the activities of their progeny are measured by gamma spectrometry (see text).

Table 5
ICP-MS results (μg/g) of Th for 4 aliquots from location **7**. The sample mean and the standard deviation of four samples are the values listed in Table 4 for sample **7**.

7–1	7–2	7–3	7–4	Sample mean (unweighted)	Standard deviation
1.966 ± 0.031	1.667 ± 0.025	1.739 ± 0.033	2.032 ± 0.047	1.85	0.18

Table 6
Gamma emitter specific activity in the water samples.

Sample Locations	^{40}K (Bq/L)	^{60}Co (Bq/L)	^{137}Cs (Bq/L)	^{208}Tl (Bq/L)	^{212}Pb (Bq/L)
1. Port Foster	8.5 ± 1.8	<0.30	<0.31	<0.33	<0.55
2. Irizar Lake	<2	<0.23	<0.20	<0.24	<0.50
3. Whalers Bay	11.4 ± 1.3	0.32 ± 0.11	0.30 ± 0.11	<0.21	<0.50
4. Fumarole Bay	10.0 ± 1.5	<0.24	<0.24	<0.26	<0.41
5. Vapour Col (Snow)	<2	<0.21	<0.21	0.66 ± 0.10	1.87 ± 0.17
6. Chilean Shelter	17.0 ± 4.0	<0.24	<0.26	<0.26	<0.41

Additionally, the analysis of gamma-ray emitting radionuclides in water samples, showed that ^{137}Cs and ^{60}Co coexist in one location, Whalers Bay. The presence of ^{137}Cs and ^{60}Co indicates anthropogenic contamination because, both radionuclides are artificial. The results were not shocking since, in this location, abundant human activities such as hunting, fishing, and even human settlements have taken place. However, it has been more than 90 years since the whaling base was closed [31], when there was no artificial production of ^{137}Cs or ^{60}Co. Most likely, ^{137}Cs and ^{60}Co in Whalers Bay water come from dissolved salts. ^{137}Cs can come from the soil (note that the sampled water is close to the contaminated soils samples **6** and **7**), from steel (note that also there is ^{60}Co in the water sample), or from any other contaminated building materials that arrived in that area after World War II.

As they were performed with soil samples, quantification studies were conducted. Nevertheless, because of the higher abundance of K in the samples, ICP-OES studies were now conducted (Table 7). The ^{40}K activities deduced from them (last column of Table 7) are compatible with the gamma spectrometry values (first column of Table 6). The obtained results show that the K concentrations in seawater at Deception Island are close to the mean value of 399.1 g/kg for the Atlantic surface waters [24] and within the range of seawater samples from the Atlantic and Pacific oceans [45]. Regarding the two freshwater samples, the K content of the Irizar lake is typical in the Antarctic lakes [33], and the K concentration in the snow sample reported here is similar to the potassium in the snow in other Antarctic regions [6,38].

Table 7
ICP-OES results of the water samples. The last column lists the specific activities (Bq/L) of ^{40}K, as deduced from the ICP-OES results.

Sample Locations	K (mg/L)	^{40}K (Bq/L)
1. Port Foster	375.9 ± 4.9	11.64 ± 0.15
2. Irizar Lake	11.71 ± 0.85	0.36 ± 0.03
3. Whalers Bay	389.8 ± 6.6	12.07 ± 0.21
4. Fumarole Bay	410.6 ± 9.7	12.71 ± 0.30
5. Vapour Col (Snow)	1.14 ± 0.07	0.035 ± 0.002
6. Chilean Shelter	377.6 ± 7.0	11.69 ± 0.22

3.4. Radionuclide activity studies in air filter samples

To increase our understanding and knowledge about the human impact on the Antarctica ecosystem, additional studies were conducted with air filter samples. The analysis of the radionuclides present in Antarctic air is a powerful tool to study the atmospheric chemistry [13], and its influence on all ecosystems and human health. For these studies, we used six air samples collected for 24 h on quartz filters, and the deposited radionuclides were measured by gamma spectrometry. The obtained results are listed in Table 8, where significant variability of the results from one day to another can be observed.

Over the Antarctic region, strong wind events are notable and play an important role in atmospheric distribution and circulation [47]. Consequently, the composition of aerosols can be drastically modified from one day to another. This fact is perfectly visible in the air mass back trajectory analysis conducted (Fig. 8), where the origin of every studied current varies from one day to another. In these studies, the influence of

Table 8
Concentration activity (mBq/m^3) of air samples for 6 days in the Spanish base "Juan Carlos I" during the 2019–2020 campaign.

Sampling date	^{214}Bi	^{214}Pb	^{212}Pb	^{208}Tl	^{137}Cs	^{60}Co	^{40}K
26/01/2020	0.40 ± 0.15	<0.20	<0.11	<0.20	0.38 ± 0.09	<0.22	<2.0
27/01/2020	2.57 ± 0.37	1.72 ± 0.31	<0.13	<0.22	<0.23	<0.30	<2.0
28/01/2020	0.90 ± 0.16	0.48 ± 0.11	<0.07	<0.20	0.29 ± 0.08	0.26 ± 0.10	1.98 ± 0.74
29/01/2020	<0.40	<0.20	0.19 ± 0.06	0.36 ± 0.12	<0.23	<0.26	<2.6
07/02/2020	<0.40	<0.40	<0.06	0.10 ± 0.06	<0.20	<0.22	3.13 ± 2.07
08/02/2020	<0.40	<0.24	<0.12	<0.20	<0.22	<0.24	3.69 ± 2.77

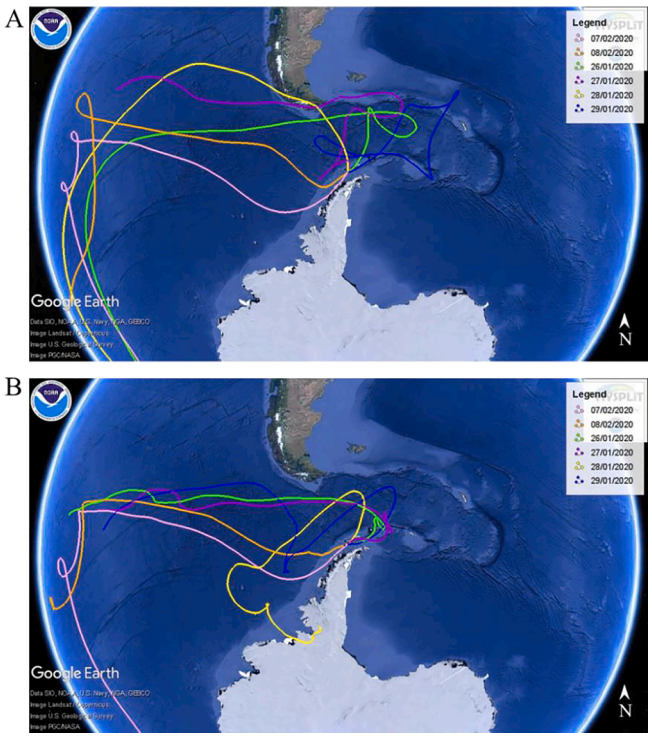

Fig. 8. Total 10-day air mass analysis of air mass back trajectories arriving at Gabriel de Castilla Station using GDAS1 dataset (Global data assimilation system) A) at a height of 542 m (highest point of Deception) B) at a height of 40 m (height of the volume sampler location).

height was evaluated and studied.

According to the calculated trajectories, when the operating wind currents only passed through the ocean, no evidences of anthropogenic radionuclides was detected (Fig. 8, lines blue/pink/orange). Nevertheless, some levels of ^{137}Cs and ^{60}Co potentially come from South America as a result of long-range transport (Fig. 8, line yellow). In addition to day 28/01/2020, the filter corresponding to day 26/01/2020 also recorded some levels of ^{137}Cs (Fig. 8, line green). According to the air mass back trajectories study conducted, some long-range transport may occur since no evidence of a local or nearby source has been observed in the period analysed.

In the studies published by Gorzkiewicz et al. in different Antarctic bases [17], they found some traces of the radionuclides presented here, but in much lower concentrations. In fact, they did not find ^{137}Cs activity concentrations above their MDC levels. Moving to a more abundant radionuclide, ^{40}K, Gorzkiewicz et al. registered an average value of 40 μBq/m^3, which is almost 50 times less than we detected.

For this reason, the distance between the volume sample collector and the soil may be not enough (1.20 m), to prevent the collector from absorbing resuspended aerosols. In these terms, this is still important because, due to their small dynamic diameter, these aerosols can potentially be breathed by humans or the rest of the Antarctic fauna.

4. Conclusions

A study on potential radioactive pollution in Deception Island (Antarctica) was conducted during this research. This study analysed the natural radioactivity in soil samples collected from different points on Deception Island. The major contributors were ^{210}Pb and ^{40}K, where *unsupported* levels of ^{210}Pb were found in two specific places, both old housing aircraft facilities. The average ^{40}K radioactivity registered (149.11 Bq/kg) was lower than the average concentration of the upper continental crust, 850 Bq/kg. However, it is consistent with the dominant rock at the sampling area. Additionally, detectable levels of anthropogenic ^{137}Cs radionuclide were found in old settlements for hunting. The specific activities obtained by gamma spectrometry combined with the mass fractions U and Th obtained by ICP-MS show that the unsupported ^{210}Pb is the only breakage of the ^{238}U chain. In terms of ^{232}Th chain, ICP-MS analysis was essential to detect the disequilibrium of the chain ^{228}Ra−^{228}Th at 3σ level.

The human radioactive pollution also spread to water, since ^{232}Th daughters were only found in the snow sample. Besides, significant levels of ^{137}Cs and ^{60}Co coexist in one particular location, Whalers Bay.

Additional analyses were conducted on air filter samples together with the air mass back trajectory studies. It is believed that the main source of the detected elements is the resuspension of local species. Antarctica is one of the last regions on Earth that remain isolated from industries and traffic, but it is still damaged and in recovering from human activities performed in the past.

The highlight of the study is the natural radioactivity in both soil, water, and air samples of the region. The study also shows anthropogenic radionuclides such as ^{60}Co and ^{137}Cs, and ^{210}Pb pollution in some places. According to this, the self-cleanness of the Antarctica seems to be not as efficient as expected, since pollution from more than 90 years remains. Therefore, more restrictive laws must be implemented to protect the Antarctic region from remote pollution and give it time to recover its unspoiled condition.

Funding

The authors gratefully acknowledge the University of Zaragoza (UZ2021-CIE-01), the Departamento de Ciencia, Universidad y Sociedad del Conocimiento del Gobierno de Aragón (E49_23R) and E27_20R), and the Ministry of Science and Innovation of Spain (CTM2017-82929-R). C. M.-M.'s work was funded by a postdoctoral contract (PRE2018-085309) granted by the Spanish government.

CRediT authorship contribution statement

E. Abás: Writing – original draft, Methodology, Formal analysis. **C. Marina-Montes:** Writing – original draft, Methodology, Formal analysis. **C. Pérez-Marín:** Methodology, Formal analysis. **J. Puimedón:** Writing – original draft, Methodology, Formal analysis. **J. Anzano:** Project administration, Funding acquisition, Supervision.

Declaration of Competing Interest

The authors declare that they have no known competing financial interests or personal relationships that could have appeared to influence the work reported in this paper.

Data availability

Data will be made available on request.

Acknowledgements

The authors would like to acknowledge the use of the Servicio General de Apoyo a la Investigación-SAI, University of Zaragoza, and especially to the Servicio de Líquidos Criogénicos. The authors also thank the military staff at the Gabriel de Castilla Spanish Antarctic Research Station for help with sample collection and installation of the equipment during 2018–2019 campaign, as well as the Juan Carlos I research staff during the 2019–2020 campaign. Figs. 1 and 8 were taken from Google Earth Pro. The authors gratefully acknowledge the NOAA Air Resources Laboratory (ARL) for providing the HYSPLIT transport and dispersion model and/or the READY website (https://www.ready.noaa.gov) used in this publication.

References

[1] Antarctic Treaty Secretariat. (https://www.ats.aq). (accessed 20th Dec 2020).
[2] M.M. Arienzo, J.R. McConnell, N. Chellman, A.S. Criscitiello, M. Curran, D. Fritzsche, S. Kipfstuhl, R. Mulvaney, M. Nolan, T. Opel, M. Sigl, J.P. Steffensen, A Method for continuous 239Pu determinations in arctic and antarctic ice cores, Environ. Sci. Tech. 50 (13) (2016) 7066–7073, https://doi.org/10.1021/acs.est.6b01108.
[3] A. Baeza, L.M. Del Rio, A. Jimenez, C. Miro, E. Navarro, J.M. Paniagua, Recent evolution of the overall radioactive levels in the ice of Livingston Island (Antarctica), Appl. Radiat. Isot. 47 (8) (1996) 811–819, https://doi.org/10.1016/0969-8043(96)00033-4.
[4] A.K. Bakshi, R. Prajith, S. Chinnaesakki, R. Pal, D. Sathian, A. Dhar, T.P. Selvam, B. K. Sapra, D. Datta, Measurements of background radiation levels around Indian station Bharati, during 33rd Indian Scientific Expedition to Antarctica, J. Environ. Radioact. (2017) 54–61. https://doi.org/10.1016/jjenvrad201611025.
[5] P. Blanco, F. Vera Tomé, J.C. Lozano, Fractionation of natural radionuclides in soils from a uranium mineralized area in the south-west of Spain, J. Environ. Radioact. 79 (2005) 315–330, https://doi.org/10.1016/j.jenvrad.2004.08.006.
[6] F. Borghini, R. Bargagli, Changes of major ion concentrations in melting snow and terrestrial waters from northern Victoria Land, Antarctica, Antarctic Sci. 16 (2) (2004) 107–115, https://doi.org/10.1017/S095410200400197X.
[7] E. Browne, R.B. Firestone, V.S. Shirley, Table of Radioactive Isotopes, John Wiley and Sons Inc, New York, 1986.
[8] K. Bunzl, W. Kracke, Natural radioactive contaminants in solder, Nucl. Instrum. Methods Phys. Res., Sect. A 238 (1985) 191–192, https://doi.org/10.1016/0168-9002(85)91049-6.
[9] M. Dowdall, J. O'Dea, 226Ra/238U disequilibrium in an upland organic soil exhibiting elevated natural radioactivity, J. Environ. Radioact. 59 (1) (2002) 91–104, https://doi.org/10.1016/S0265-931X(01)00038-8.
[10] M. Dowdall, Ø.G. Selnaes, J.P. Gwynn, C. Davids, Simultaneous determination of 226Ra and 238U in soil and environmental materials by gamma-spectrometry in the absence of radium progeny equilibrium, J. Radioanal. Nucl. Chem. 261 (3) (2004) 513–521, https://doi.org/10.1023/B:JRNC.0000037091.19952.d3.
[11] C. Dueñas, M.C. Fernández, J. Carretero, E. Liger, M. Pérez, Release of 222Rn from some soils, Ann. Geophys. 15 (1997) 124–133, https://doi.org/10.1007/s00585-997-0124-0.
[12] C. Dueñas, M.C. Fernández, E. Gordo, S. Cañete, M. Pérez, Chemical and radioactive composition of bulk deposition in Málaga (Spain), Atmos. Environ. 62 (2012) 1–8, https://doi.org/10.1016/j.atmosenv.2012.07.073.
[13] H.W. Gäggeler, Radioactivity in the atmosphere, Radiochim. Acta 70–71 (s1) (1995) 345–354, https://doi.org/10.1524/ract.1995.7071.s1.345.
[14] M. García-Talavera, Evaluation of the suitability of various γ lines for the γ spectrometric determination of 238U in environmental samples, Appl. Radiat. Isot. 59 (2003) 165–173, https://doi.org/10.1016/S0969-8043(03)00153-2.
[15] J.M. Godoy, L.A. Schuch, D.J.R. Nordemann, V.R.G. Reis, M. Ramalho, J.C. Recio, R.R.A. Brito, M.A. Olech, 137Cs, 226, 228Ra, 210Pb and 40K concentrations in Antarctic soil, sediment and selected moss and lichen samples, J. Environ. Radioact. 41 (1) (1998) 33–45, https://doi.org/10.1016/S0265-931X(97)00084-2.
[16] Gordon, M.S., Rodbell, K.P., Heidel, D.F., Murray, C.E., Tang, H.H.K., Dwyer-McNally, B., Warburton, W.K., 2010. Alpha-Particle Emission Energy Spectra From Materials Used for Solder Bumps. IEEE Transactions on Nuclear Science, VOL. 57, NO. 6, 57(6), 3251. https://doi.org/10.1109/TNS.2010.2085015.
[17] K. Gorzkiewicz, R. Kierepko, J. Paatero, A. Virkkula, J.W. Mietelski, Air radioactivity in Marambio Base: The peculiar character of Antarctic Peninsula, J. Environ. Radioact. 251–252 (2022), 106930, https://doi.org/10.1016/j.jenvrad.2022.106930.
[18] W.C. Graustein, K.K. Turekian, Radon fluxes from soils to the atmosphere measured by 210Pb-226Ra disequilibrium in soils, Geophys. Res. Lett. 17 (6) (1990) 841–844, https://doi.org/10.1029/92RG00055.
[19] G. Heusser, Low-radioactivity background techniques, Annu. Rev. Nucl. Part. Sci. 45 (1995) 543–590, https://doi.org/10.1146/annurev.ns.45.120195.002551.
[20] IAATO, 2017. Report on IAATO Operator Use of Antarctic Peninsula Landing Sites and ATCM Visitor Site Guidelines, 2016-17 Season. IP 164. https://iaato.org/es/past-iaato-information-papers.
[21] M. Ivanovich, Uranium series disequilibrium: concepts and applications, Radiochim. Acta 64 (1994) 81–94.
[22] C. Marina-Montes, L.V. Pérez-Arribas, M. Escudero, J. Anzano, J.O. Cáceres, Heavy metal transport and evolution of atmospheric aerosols in the Antarctic region, Sci. Total Environ. 721 (2020), 137702, https://doi.org/10.1016/j.scitotenv.2020.137702.
[23] J.W. Mietelski, M.A. Olech, K. Sobiech-Matura, B.J. Howard, P. Gaca, M. Zwolak, S. Błażej, E. Tomankiewicz, 137Cs, 40K, 238Pu, 239+240Pu and 90Sr in biological samples from King George Island (Southern Shetlands) in Antarctica, Polar Biol. 31 (9) (2008) 1081–1089, https://doi.org/10.1007/s00300-008-0449-5.
[24] F.J. Millero, R. Feistel, D.G. Wright, T.J. McDougall, The composition of standard seawater and the definition of the reference-composition salinity scale, Deep-Sea Research I 55 (2008) 50–72, https://doi.org/10.1016/j.dsr.2007.10.001.
[25] N. Mitchell, D. Pérez-Sánchez, M.C. Thorne, A review of the behaviour of U-238 series radionuclides in soils and plants, J. Radiol. Prot. (2013) R17–R48, https://doi.org/10.1088/0952-4746/33/2/R17.
[26] M.O. Naumenko, K. Mezger, T.F. Nägler, I.M. Villa, High precision determination of the terrestrial 40K abundance, Geochim. Cosmochim. Acta 122 (2013) 353–362, https://doi.org/10.1016/j.gca.2013.08.019.
[27] A. Navas, J. Soto, J. López-Martínez, Radionuclides in soils of Byers Peninsula, South Shetland Islands, Western Antarctica, Appl. Radiat. Isotopes 62 (5) (2005) 809–816, https://doi.org/10.1016/j.apradiso.2004.11.007.
[28] A. Navas, J. Soto, J. Machín, 238U, 226Ra, 210Pb, 232Th and 40K activities in soil profiles of the Flysch sector (Central Spanish Pyrenees), Appl. Radiat. Isot. 57 (2002) 579–589, https://doi.org/10.1016/S0969-8043(02)00131-8.
[29] W.W. Nazaroff, Radon transport from soil to air, Rev. Geophys. 30 (2) (1992) 137–160, https://doi.org/10.1029/92RG00055.
[30] R. Pal, A.C. Patra, A.K. Bakshi, B. Dhabekar, P.J. Reddy, P. Sengupta, B.K. Sapra, Investigations on baseline levels for natural radioactivity in soils, rocks, and lakes of Larsemann Hills in East Antarctica, Environ. Monit. Assess. 193 (12) (2021) 822, https://doi.org/10.1007/s10661-021-09446-8.
[31] M. Pearson, A. Zarankin, M.A. Salerno, Chapter 14 - Exploring and exploiting Antarctica: The early human interactions, in: M. Oliva, J. Ruiz-Fernández (Eds.), Past Antarctica, Academic Press, 2020, pp. 259–278, https://doi.org/10.1016/B978-0-12-817925-3.00014-8.
[32] Picciotto, E., Wilgain, S., 1963. Fission products in Antarctic snow, A reference level for measuring accumulation. J. Geophys. Res. (1896-1977) 68(21), 5965-5972. https://doi.org/10.1029/JZ068i021p05965.
[33] C. Porcino, Azzaro, A review on the geochemistry of lakes in Victoria Land (Antarctica), Chemosphere 251 (2020), 126229, https://doi.org/10.1016/j.chemosphere.2020.126229.
[34] M. Pourchet, S.K. Bartarya, M. Maignan, J. Jouzel, J.F. Pinglot, A.J. Aristarain, G. Furdada, V.M. Kotlyakov, E. Mosley-Thompson, N. Preiss, N.W. Young, Distribution and fall-out of 137Cs and other radionuclides over Antarctica, J. Glaciol. 43 (145) (1997) 435–445, https://doi.org/10.3189/S0022143000035024.
[35] Pourchet, M., Magand O Fau - Frezzotti, M., Frezzotti M Fau - Ekaykin, A., Ekaykin A Fau - Winther, J.G., Winther, J.G., 2003. Radionuclides deposition over Antarctica. J. Environ Radioact 68(2), 21. https://doi.org/10.1016/S0265-931X(03)00055-9.
[36] P.P. Povinec, P. Vojtyla, J.F. Comanducci, Monte Carlo simulation of background characteristics of gamma-ray spectrometers—a comparison with experiment, Radioactivity Environ. 11 (2008) 163–208, https://doi.org/10.1016/S1569-4860(07)11005-6.
[37] X. Querol, A. Alastuey, A. Lopez-Soler, E. Mantilla, F. Plana, Mineral composition of atmospheric particulates around a large coal-fired power station, Atmos. Environ. 30 (21) (1996) 3557–3572, https://doi.org/10.1016/1352-2310(96)00108-2.
[38] A.M. Rankin, E.W. Wolff, Ammonium and potassium in snow around an emperor penguin colony, Antarct. Sci. 12 (2) (2000) 154–159, https://doi.org/10.1017/S0954102000000201.
[39] Standardization, E.C.f., 2014. EN 12341: 2014. Ambient air—Standard gravimetric measurement method for the determination of the PM10 or PM2, 5 mass concentration of suspended particulate matter. CEN. European Committee for Standardization Brussels, Belgium.
[40] G. Steinhauser, A. Brandl, T.E. Johnson, Comparison of the Chernobyl and Fukushima nuclear accidents: A review of the environmental impacts, Sci. Total Environ. 470–471 (2014) 800–817, https://doi.org/10.1016/j.scitotenv.2013.10.029.
[41] K.M. Szufa, J.W. Mietelski, M.A. Olech, A. Kowalska, K. Brudecki, Anthropogenic radionuclides in Antarctic biota – dosimetrical considerations, J. Environ. Radioact. 213 (2020), 106140, https://doi.org/10.1016/j.jenvrad.2019.106140.
[43] W.R. Van Schmus, Natural Radioactivity of the Crust and Mantle, in: T.J. Ahrens (Ed.), Global Earth Physics: A Handbook of Physical Constants, Volume 1, American Geophysical Union, 1995, pp. 283–291.
[44] K.-M. Wai, D. Krstic, D. Nikezic, T.-H. Lin, P.K.N. Yu, External Cesium-137 doses to humans from soil influenced by the Fukushima and Chernobyl nuclear power plants accidents: a comparative study, Sci. Rep. 10 (1) (2020) 7902, https://doi.org/10.1038/s41598-020-64812-9.
[45] K. Wang, H.G. Close, B. Tuller-Ross, H. Chen, Global average potassium isotope composition of modern seawater, ACS Earth Space Chem. 4 (2020) 1010–1017, https://doi.org/10.1021/acsearthspacechem.0c00047.
[46] H. Yang, P.G. Appleby, Use of lead-210 as a novel tracer for lead (Pb) sources in plants, Sci. Rep. 6 (1) (2016) 21707, https://doi.org/10.1038/srep21707.
[47] L. Yu, S. Zhong, Strong wind speed events over antarctica and its surrounding oceans, J. Clim. 32 (12) (2019) 3451–3470, https://doi.org/10.1175/JCLI-D-18-0831.1.
[48] X. Zou, S. Hou, K. Liu, J. Yu, W. Zhang, H. Pang, R. Hua, P. Mayewski, Uranium record from a 3 m snow pit at Dome Argus, East Antarctica, PLoS One 13 (10) (2018) e0206598.
[49] Recycling and Reuse of Materials Arising from the Decommissioning of Nuclear Facilities, Radioactive Waste Management, OECD Publishing, Paris. https://doi.org/10.1787/9789264281271-en.